Simulation-Based Optimization of a Near-Infrared Spectroscopic Subcutaneous Fat Thickness Measuring Device

Robert Morhard[1,2], Heather Jeffery[1] and Alistair McEwan[1]

Abstract— **Using Monte Carlo simulations we optimized the wavelength and source-detector distance (SDD) of a reflectance-based spectroscopic device used for measuring subcutaneous fat thickness. As the optical properties of muscle, fat and dermis are wavelength dependent, it is necessary to choose a wavelength that is highly sensitive to fat but insensitive to water and melanin. The SDD is important since it determines average photon penetration depth. With a tissue optics plug-in for the GEANT4/GAMOS system and published ex vivo tissue optical properties we were able to predict the behavior of different device configurations when used with varying thicknesses of fat, melanin concentrations or hydration levels. Our results indicate that the ideal wavelengths for fat measurement are 630-650 nm with an SDD of 2.6-29 cm. We also examined the potential of using near infrared (NIR) spectroscopy to determine tissue hydration levels, but concluded that this wavelength range was not ideal.**

INTRODUCTION

There is a demand for a cheap, accurate, noninvasive fat measurement in various fields such as the diagnosis of infantile malnutrition in developing countries, in-home body fat assessment and proper calibration of skin surface near-infrared spectroscopy diagnostics of blood constituents. Currently techniques are available to measure body fat, but they are either expensive, bulky, require extensive training or inaccurate. The gold standard techniques with the highest accuracy are air displacement plethysmography (PEAPOD or BODPOD), dual-energy X-ray absorptiometry (DXA) and hydrostatic weighing [1]. While increasing the accuracy of these instruments is an active area of research, many applications require more portable and reasonably priced alternatives.

Measuring subcutaneous fat thickness is necessary for critical health and wellbeing applications in which it can confound readings of tissues that lie beneath it [2]. Accurate fat thickness measurements could increase the accuracy of techniques such as pulse oximetry, vein finding for cannulation and optoacoustic imaging. For applications which directly measure fat thickness, such as body composition, it has been shown that there is a high correlation between subcutaneous fat thickness and overall fat mass in both newborns [3] and adults [4].

Our primary focus is to aid in the diagnosis of infantile malnutrition in resource-limited settings. A recent study reported that over one-third of all child deaths are attributed to malnutrition [5]. The optimization will be centered on the clinically determined threshold for neonatal health of 5 mm of fat [6].

In resource-limited settings, skinfold thickness testing via calipers and anthropometric statistics are the most common measurement techniques [7]. Skinfold thickness testing can be reasonably accurate, but requires sufficient training [8]. Anthropometric statistics such as weight and length are frequently used with moderate accuracy [9], but this can also require excessive training and equipment [10]. Bioelectrical impedance analysis is a recently developed technique that is relatively inexpensive and easy-to-use, but is not more accurate than using solely anthropometric statistics in some cases [11]. NIR spectroscopy is noninvasive, cheap and has the potential to be highly accurate [4].

To date, there have been no studies that analytically optimize the geometry and spectroscopic specifications of a NIR-based body fat thickness measurement device. Given the high absorption coefficient of water [12], the high tissue water content [13] and the variance in total body water composition [14], it is important to minimize the impact on fat thickness readings. Melanin is also a strong absorber [15] and can confound readings by varying with body location and between individuals [16].

As shown in Figure 1, muscle and fat have distinct, wavelength-dependent absorption and scattering spectrums. In order to determine the thickness of fat, the amount of light reflected back out of the skin is measured. This is done with a source LED and a photodetector. From the amount of reflected light, it is possible to determine how much fat or muscle has interacted with the light since it left the source LED. The distance between the LED and the detector, determines the average photon penetration depth [17], and therefore the composition of tissue it has traveled through. In order to optimize this process, it is necessary to use a wavelength and source-detector distance with a large difference in reflectance relative to fat thickness changes and a low difference in reflectance relative to hydration and melanin changes.

Published optical properties of ex vivo tissues [18], water [12] and melanin [15] allow for accurate simulation and optimization. Our primary hypothesis was that we would be able to optimize the source-detector distance and wavelength combination for the measurement of fat thickness. Additionally we looked at device specifications to optimize hydration sensitivity in order to determine total body water. We did not look at optimizing melanin sensitivity as that has limited clinical relevance. In order to find the optimal design, we used a Monte Carlo simulation to simulate the photon transport in multi-layered biological media between a source and detector [19], [20].

978-1-4244-7929-0/14/$26.00 ©2014 IEEE

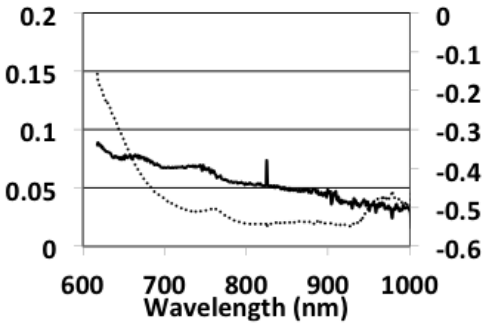

Fig. 1. Difference in muscle and fat absorption (dotted, left axis) and scattering (solid, right axis) coefficients in inverse centimeters.

MATERIALS AND METHODS

Scattering and absorption coefficients

In order to predict the reflectance of a layered system it is first necessary to know the optical coefficients of each layer. The scattering (μ_s) and absorption (μ_a) coefficients quantify the average number of scattering or absorption phenomena per unit path length of photon travel. In order to take into account the anisotropy of scattering (g), or whether scattered particles predominately continue forward (g=1), backward (g=-1) or uniformly in all directions (g=0), the reduced scattering coefficient (μ_s') is used. This value is calculated as the product of μ_s and (1-g).

Hydration modulation

In order to assess hydration sensitivity it was necessary to simulate the affect of varying tissue water content on optical properties. This was done using equations 1-3.

$$\mu_{abs,f,hydr} = \alpha_f \tau \mu_{abs,water} + (1 - \alpha_f \tau) \cdot \mu_{abs,f} \quad (1)$$

$$\mu_{abs,m,hydr} = \alpha_m \tau \mu_{abs,water} + (1 - \alpha_m \tau) \cdot \mu_{abs,m} \quad (2)$$

$$\mu_{abs,d,hydr} = \alpha_d \tau \mu_{abs,water} + (1 - \alpha_d \tau) \cdot \mu_{abs,d} \quad (3)$$

where $\mu_{abs,x,hydr}$ is the new absorption coefficient for fat (f), muscle (m) or dermis (d) with a new hydration level,$\alpha_x$is the average water composition (65% for dermis, 20% for fat and 75% for muscle [23]), τ is the change in hydration level (.05 is 5% more than average, -.05 is 5% less than average), $\mu_{abs,water}$ is the absorption profile for water [12] and $\mu_{abs,x}$ is the absorption profile of muscle, fat or dermis [18]. These equations generate new coefficients of absorption which are then fed into the Monte Carlo simulations to estimate the effect of hydration changes. While they may deviate from the actual reflectance values, our hypothesis is that they should represent the relative changes in the reflectance profiles.

Refractive index determination

The refractive indices for tissue are also wavelength dependent. The values for fat and muscle are based off the Cauchy coefficients calculated for porcine models [21]. In the absence of wavelength-dependent refractive index data for dermis the value was assumed to be 1.4 [22].

GAMOS/GEANT4 Tissue- Optics Plug in

We use Monte Carlo simulations to predict the number of photons that will reach the detector. This is ideal because the scattering and absorption coefficients essentially represent probabilities and by running many simulations we can estimate the expected number of photons to reach the detector for a given system.

The layout of our model is shown in Figure 2. The underlying green layer is muscle. The blue layer is fat with a thickness that changes from 1mm to 10mm throughout a simulation. The white layer is a layer of dermis that is 1.2 mm thick [23]. The red box is a 5 mm by 5 mm detector that reports hits. Photons enter the very center of the model. By altering the optical properties of these layers (to represent hydration changes), the thickness of fat, type of dermis (Caucasian or Negroid) and the source-detector distance, it is possible to collect the necessary data to optimize this technique.

Model specifications

In order to acquire the necessary data for optimization, the Monte Carlo simulations were run on models with Caucasian dermis and normal hydration from 1 to 10 mm of fat in increments of 1 mm, Negroid dermis with normal hydration and 5 mm of fat and dehydrated (-20%) and hydrated (20%) Caucasian dermis with 5 mm of fat. Each simulation examined source-detector separations of 1.5 to 2.9 cm in increments of 0.1 cm and wavelengths from 620 to 1000 nm in increments of 10 nm. The number of photons simulated was $8{\cdot}10^6$. Source-detector distance in this range were examined as they will produce average photon penetration depths on the order of 5 mm for the wavelengths considered [17].

Normalization

In order to properly assess the signal, each term in Equation 4 is divided by the number of photons to reach the detector for a normally hydrated, Caucasian-dermis system with 5 mm of fat for each wavelength/SDD combination. Smaller SDDs have stronger signals and therefore all the signal statistics are higher.

Optimization Procedure

The optimal wavelength and source-detector distance combination will have a high sensitivity to fat thickness changes, a constant change in signal with respect to fat thickness, and a low sensitivity to hydration and melanin changes. The goal is to optimize this value:

$$V_F = \left(\frac{\delta S}{\delta Fat}\right) - \sum (\hat{S}_F - S_{F,n})^2 - \left(\frac{\delta S}{\delta Hdr}\right) - \left(\frac{\delta S}{\delta Mel}\right) \quad (4)$$

$$(\lambda_F, SDD_F) = max_{\lambda,SDD}(V_F) \quad (5)$$

where S is the count of photons to reach the detector, $\hat{S}_F$ is the average change in counts per mm change in fat and $S_{F,n}$ is the change in counts from thickness n-1 mm to thickness n mm. The first term is the mean signal change relative to fat thickness and the second term represents the variance in this signal change at different thicknesses. Optimizing based on these two terms will give the ideal specifications for fat detection without taking into account the confounding influence of hydration (Hdr) or melanin (Mel) changes. The third and fourth terms represent these

influences. λ_F and SDD_F are the optimal wavelength and source-detector distance, respectively. If, via another LED or separate measurement technique, hydration level is known, then it is not necessary to include the third term. The same is true for melanin measurement and the fourth term. Excluding the third or fourth term in optimization will simulate the knowledge of these factors.

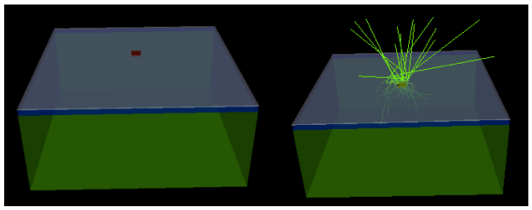

Fig. 2. Left is an overview of the simulation geometry. The bottom green layer is muscle (8 cm thick), the blue layer is fat (varying from 1 to 10 mm thick), the white layer is dermis (1.2 mm thick) and the red box is the detector. Right is a side view of the model with the photon traces in bright green either terminating with absorption in the tissue or scattering out as reflection.

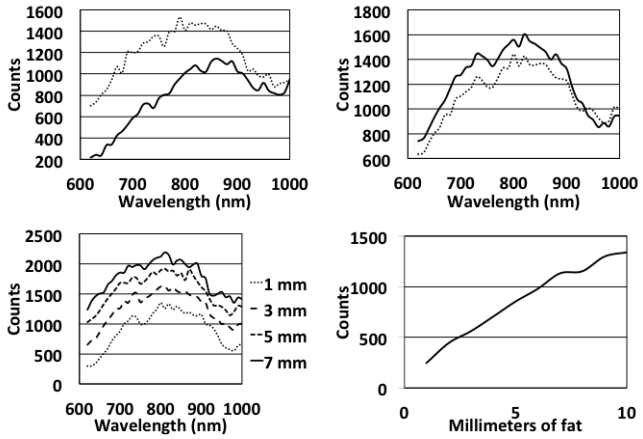

Fig. 3. Top left is a comparison of the number of photons to reach the detector between systems with Caucasian (dotted) and Negroid (solid) dermis on top of 5 millimeters of fat and muscle. Top right is a comparison between hydrated (solid) and dehydrated (dotted) Caucasian systems. Bottom left is a comparison between a system with 1 millimeter of fat and 10 millimeters of fat under Caucasian dermis. Bottom right is a typical plot of the detector behavior for varying fat thicknesses under Caucasian dermis.

In order to assess the efficacy of Equations 4-5 we must calculate the error rates and sensitivities. Equation 6 calculates the error (Err_F) in fat-reading respective to hydration change in units of $\frac{counts}{\%\, hydration}$. This is the dependence of the optimal fat-reading configuration on hydration changes.

$$Err_F = \sum \frac{S(20\%, t, \lambda_F, SDD_F) - S(-20\%, t, \lambda_F, SDD_F)}{n \cdot 40\%\, Hydration} \quad (6)$$

S is the signal and depends on hydration level, mm of fat (t), wavelength and source-detector distance. The variable n represents the hydration levels (n = 1 refers to -20% hydration change, n =2 refers to 0% hydration change and n=3 refers to +20% hydration change). Equation 7 calculates the sensitivity (Sen_F) of the optimal fat-reading configuration for fat thickness in terms of $\frac{counts}{mm\ of\ fat}$

TABLE I

FAT OPTIMIZATION VALUES WITHOUT MELANIN

Wavelength (nm)	630	650	640
SDD (cm)	2.9	2.8	2.6
V_f	0.157	0.148	0.140
Normalized Fat Sensitivity	0.252	0.218	0.201
Normalized Fat Signal Std Dev	0.089	0.065	0.055
Normalized Hydration Sensitivity	0.0059	0.0057	0.0055
Normalized Melanin Sensitivity	0.029	0.009	0.025
Hydration Bias	0.023	0.026	0.028
Melain Bias	2.89	2.77	3.18

TABLE II

FAT OPTIMIZATION VALUES WITH MELANIN

Wavelength (nm)	1000	980	980
SDD (cm)	1.9	2.4	2.5
V_f	0.063	0.051	0.033
Normalized Fat Sensitivity	0.093	0.151	0.130
Normalized Fat Signal Std Dev	0.029	0.0509	0.0782
Normalized Hydration Sensitivity	0.0013	0.0013	0.0011
Normalized Melanin Sensitivity	0.0	0.0474	0.0175
Hydration Bias	-0.014	-0.0120	-0.087
Melain Bias	0.0	-0.314	-0.134

$$Sen_F = \sum_n \frac{S(0\%, n+1, \lambda_F, SDD_F) - S(0\%, n, \lambda_F, SDD_F)}{n \cdot mmfat} \quad (7)$$

In this case, n refers to the thickness of fat (n = 1 refers to 1 mm of fat).

$$Bias_F = \frac{Error_F}{Sensitivity_F} \quad (8)$$

Equation 8 calculates the error in fat-reading due to hydration changes in terms of $\frac{mm\ of\ fat}{\%\, hydration}$. Melanin-related error and bias are calculated in a similar manner, but with the difference between Caucasian and Negroid models.

RESULTS

The results for different system parameters are shown in Figure 3. If only the first 3 terms of Equation 4 are taken into account (and the influence of melanin is neglected), the optimal specifications are estimated to be 630 nm at a separation of 2.9 cm. These results are summarized in Table 1. Values are given as a fraction of total signal for a normally hydrated system with Caucasian dermis and 5 mm of fat. The biases are in terms of either $\frac{mm\ of\ fat}{\%\, hydration}$ or $\frac{mm\ of\ fat}{melanin\ change}$. If all four terms from equation 4 are taken into account, the optimal combinations are shown in Table 2. Neglecting the third term doesn't change the results in Table 1 due to the low absorption coefficient of water in this range [12].

DISCUSSION

By optimizing Equations 4-7, we found the ideal detection wavelength and source-detection distance to measure fat thickness. Accurately measuring fat thickness is in diagnosing malnutrition or dehydration, analyzing body composition or in calibrating other spectroscopic devices. We did not look at measuring melanin concentration as this seems to have limited clinical applicability, but the previously mentioned equations could be used to this end.

The ideal wavelengths for fat measurement, without considering melanin, are 630, 650 and 640 nm with respective source detector separations of 2.9, 2.8 and 2.6 cm. At this region, a 1% change in hydration should cause an error in fat thickness sensing of approximately .02 mm. The difference between Table 1 and Table 2 demonstrates the large impact of melanin variance of fat assessment. Therefore it is either necessary to calculate curves for individual ethinc groups, determine melanin content with another LED, measure in photoprotected areas [16] (areas not exposed to the sun), or restrict use to neonates (who tend to have lower melanin concentrations). If the hydration bias proves to be larger than predicted, it could be measured with another LED and adjust the fat prediction algorithm accordingly.

Looking at wavelengths outside the 600 to 1000 nm range could be helpful, especially to increase hydration sensitivity. In order to do this it will be necessary to examine more ex vivo tissue as their precise optical properties are unknown. Creating a more complex simulation with bone and epidermis would also increase the clinical relevance of these models. Additional research is necessary to determine which location yields the highest correlation between subcutaneous fat thickness and total body fat.

CONCLUSION

In this study we used published tissue optical coefficients and Monte-Carlo-based particle tracking simulations to optimize the design of a device to measure subcutaneous fat thickness. The ideal wavelength for fat detection is 630 nm with a source-detector distance of 2.9 cm without considering the effect of melanin and 1000 nm with a separation of 1.9 cm if melanin is considered. Using the results from these simulations as a foundation for in vivo spectroscopic measurements calibrated against a gold standard, such as a PEAPOD or BODPOD, would be the most efficient next step in designing a cheap, optimally accurate and non-invasive fat thickness measurement device. While this simulation-based optimization will be useful in guiding in-vivo optimization trials, it has limited utility without them as it is based on a simplified model of the skin structure.

ACKNOWLEDGEMENTS

The authors acknowledge the support of the Bill and Melinda Gates Foundation Grand Challenges Scheme. Dr. Peter Jones and Fatin Hamimi have provided vital assitance. Additionally the authors acknowledge Dr. Pedro Arce and Adam Glaser for their continuous and patient support with GAMOS installation and instruction.

REFERENCES

[1] D. Brodie, V. Moscrip and R. Hutcheon, Body composition measurement: a review of hydrodensitometry, anthropometry, and impedance methods, Nutrition, vol. 14, pp. 296-310, 1998.

[2] M.C.P. Van Beekvelt and B.G.M. Van Engelen, Adipose tissue thickness affects in vivo quantitative near-IR spectroscopy in human skeletal muscle, Clinical Science, vol. 101, pp. 21-28, 2001.

[3] T.A. Harrington, E.L Thomas, G. Frost, N. Modi and J.D. Bell, Distribution of adipose tissue in the newborn, Pediatric Research, vol. 55, pp. 437-441, 2004.

[4] J.M. Conway, K.H. Norris and C.E. Bodwell, A new approach for the estimation of body composition: infrared interactance, The American Journal of Clinical Nutrition, vol. 40, pp. 1123-1130, 1984.

[5] UNICEF. Facts for life. New York: United Nations Childrens Fund, 2010

[6] F. Gardeil, R. Green, B. Stuart and M.J. Turner, Subcutaneous Fat in the Fetal Abdomen as a Predictor of Growth Restriction, Obstetrics and Gynecology, vol. 94, no. 2, pp. 209-212, 1999.

[7] M. Onis, eliability of anthropometric measurements in the WHO Multicentre Growth Reference Study, Acta Paediatrica, vol. 95, pp. 38-46, 2006.

[8] K. Klipstein-Grobusch, T. Georg and H. Boeing, Interviewer variability in anthropometric measurements and estimates of body composition, International journal of epidemiology, vol. 26, pp. Supplementary S174-180, 1997.

[9] O.J. Adebami and J.A. Owa, Comparison between CANSCORE and other anthropometric indicators in fetal malnutrition, The Indian Journal of Pediatrics, vol. 75, pp. 439-442, 2008.

[10] A.J. Wood, C.H. Raynes-Greenow, A.E. Carberry and H.E. Jeffery, Neonatal length inaccuracies in clinical practice and related percentile discrepancies detected by a simple length-board, Journal of Paediatrics and Child Health, vol. 49, pp. 199-203, 2013.

[11] B.E. Lingwood, A.M. Storm van Leeuwen, A.E. Carberry, E.C. Fitzgerald, L.K. Callaway, P.B. Colditz, et al., Prediction of fat-free mass and percentage of body fat in neonates using bioelectrical impedance analysis and anthropometric measures: validation against the PEA POD. The British Journal of Nutrition, vol. 107, pp. 1545-1552, 2012.

[12] G. M. Hale and M.R. Querry, Optical Constants of Water in the 200-nm to 200-μm Wavelength Region, Applied Optics, vol. 12, pp. 555-563, 1973.

[13] H.Q. Woodard and D.R. White, The composition of body tissues, The British Journal of Radiology, vol. 59, pp. 1209-1218, 1986.

[14] H.P. Sheng and R.A. Huggins, A review of body composition studies with emphasis on total body water and fat, The American Journal of Clinical Nutrition, vol. 32, pp. 630-647, 1979.

[15] Sarna T, Swartz HA. The Physical Properties of Melanins. The Pigmentary System: Blackwell Publishing Ltd; 2007. p. 311-41. T. Sarma and H.A. Swartz, The Physical Properties of Melanins. The Pigmentary System: Blackwell Publishing Ltd, pp. 311-41, 2007.

[16] S. Alaluf, D. Atkins, K. Barrett, M. Blount, N. Carter and A. Heath, Ethnic Variation in Melanin Content and Composition in Photoexposed and Photoprotected Human Skin, Pigment Cell Research, vol. 15, pp. 112-118, 2002.

[17] M.S. Patterson, S. Andersson-Engels, B.C. Wilson and E.K. Osei, Absorption spectroscopy in tissue-simulating materials: a theoretical and experimental study of photon paths, Applied Optics, vol. 34, pp. 22-30, 1995.

[18] C.R. Simpson, M. Kohl, M. Essenpreis and M. Cope, Near-infrared optical properties of ex vivo human skin and subcutaneous tissues measured using the Monte Carlo inversion technique. Physics in Medicine and Biology, vol. 43, pp. 2465-2478, 1998.

[19] A.K. Glaser, S.C. Kanick, R. Zhang, P. Arce and B.W. Pogue, A GAMOS plug-in for GEANT4 based Monte Carlo simulation of radiation-induced light transport in biological media. Biomedical Optics Express, vol. 4, pp. 4741-4759, 2013.

[20] P. Arce, P. Rato, M. Canadas and J.I. Lagares, GAMOS: A Geant4-based easy and flexible framework for nuclear medicine applications. Nuclear Science Symposium Conference Record, NSS 2008 IEEE. pp. 3163-3168, 2008.

[21] S. Cheng, H.Y. Shen, G. Zhang and C.H. Huang, Measurement of the refractive index of biotissue at four laser wavelengths. Photonics Asia 2002: International Society for Optics and Photonics, pp. 172-176, 2002.

[22] G.J. Tearney, M.E. Brezinski, B.E. Bouma, M.R. Hee, J.F. Southern and J.G. Fujimoto, Determination of the refractive index of highly scattering human tissue by optical coherence tomography, Optics Letters, vol. 20, pp. 2258-2260, 1995.

[23] M. Gniadecka and B. Quistorff. Assessment of dermal water by high-frequency ultrasound: comparative studies with nuclear magnetic resonance, British Journal of Dermatology, vol. 35, pp. 218-224, 1996.